Integrated transcriptomic and proteomic analysis of pathogenic mycobacteria and their esx-1 mutants reveal secretion-dependent regulation of ESX-1 substrates and WhiB6 as a transcriptional regulator
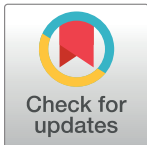
Abdallah M. Abdallah[1]☯*, **Eveline M. Weerdenburg**[2]☯, **Qingtian Guan**[1], **Roy Ummels**[2],
Stephanie Borggreve[2], **Sabir A. Adroub**[1], **Tareq B. Malas**[1], **Raeece Naeem**[1],
Huoming Zhang[3], **Thomas D. Otto**[4], **Wilbert Bitter**[2‡]*, **Arnab Pain**[1‡]*

1 Pathogen Genomics Laboratory, BESE Division, King Abdullah University of Science and Technology
(KAUST), Thuwal-Jeddah, Kingdom of Saudi Arabia, 2 Department of Medical Microbiology and Infection
Control, VU University Medical Center, Amsterdam, The Netherlands, 3 Bioscience Core Laboratory, King
Abdullah University of Science and Technology (KAUST), Thuwal-Jeddah, Kingdom of Saudi Arabia,
4 Pathogen Genomics, The Wellcome Trust Sanger Institute, Hinxton, Cambridge, United Kingdom

☯ These authors contributed equally to this work.
‡ These authors also contributed equally to this work.
* abdallah.abdallah@kaust.edu.sa (AMA); w.bitter@vumc.nl (WB); arnab.pain@kaust.edu.sa (AP)

OPEN ACCESS

Abstract

The mycobacterial type VII secretion system ESX-1 is responsible for the secretion of a
number of proteins that play important roles during host infection. The regulation of the
expression of secreted proteins is often essential to establish successful infection. Using
transcriptome sequencing, we found that the abrogation of ESX-1 function in *Mycobacterium marinum* leads to a pronounced increase in gene expression levels of the *espA* operon
during the infection of macrophages. In addition, the disruption of ESX-1-mediated protein
secretion also leads to a specific down-regulation of the ESX-1 substrates, but not of the
structural components of this system, during growth in culture medium. This effect is
observed in both *M. marinum* and *M. tuberculosis*. We established that down-regulation of
ESX-1 substrates is the result of a regulatory process that is influenced by the putative transcriptional regulator *whib6*, which is located adjacent to the *esx-1* locus. In addition, the
overexpression of the ESX-1-associated PE35/PPE68 protein pair resulted in a significantly
increased secretion of the ESX-1 substrate EsxA, demonstrating a functional link between
these proteins. Taken together, these data show that WhiB6 is required for the secretion-
dependent regulation of ESX-1 substrates and that ESX-1 substrates are regulated independently from the structural components, both during infection and as a result of active
secretion.

Introduction

Mycobacteria use several different type VII secretion systems (T7S) to transport proteins across their thick and waxy cell envelopes. One of these T7S systems, ESX-1, is responsible for the transport of a number of important virulence factors. Disruption of the *esx-1* gene cluster severely reduces the virulence of *Mycobacterium tuberculosis* [1], whereas restoration of *esx-1* in the *Mycobacterium bovis*-derived vaccine strain BCG, which lacks part of the *esx-1* region due to continuous passaging, leads to increased virulence [2]. Many studies have attempted to elucidate the function of ESX-1 substrates in virulence. In the case of pathogenic mycobacteria, such as *M. tuberculosis* and the fish pathogen *Mycobacterium marinum*, ESX-1 is responsible for the translocation of the bacteria from the phagolysosomal compartments to the cytosols of macrophages [3–5]. This translocation activity has been attributed to the ESX-1 substrate EsxA (previously also known as ESAT-6) [6, 7]. Interestingly, a closely related homologue of this protein is also secreted by non-pathogenic and non-translocating mycobacteria, such as *Mycobacterium smegmatis*. A report indicated that, although the EsxA proteins of *M. smegmatis* and *M. tuberculosis* are highly homologous, the membrane lysis potentials of these proteins are different [8]. In *M. smegmatis*, ESX-1 is involved in a completely different process, *i.e.*, conjugative DNA transfer [9]. The direct involvement of EsxA in phagosomal rupture is not undisputed, a recent report indicated that ESX-1–mediated cell lysis occurs through gross disruptions at points of bacterial contact and not through pore formation by EsxA (5). Interestingly, there are more differences between pathogenic and non-pathogenetic mycobacteria, one of which is the presence/absence of the *espACD* operon, which is exclusively present in mycobacterial species that were shown to be able to induce phagosomal rupture in host-phagocytes such as *M. kansasii* Type I, *M. bovis*, *M. tuberculosis* [10]. Possibly also other ESX-1 substrates are involved in membrane disruption. However, these other substrates could also be involved in other proposed functions of ESX-1 in pathogenic mycobacterial species, including host cell entry and intercellular spread [11–13].

The *esx-1* locus contains both genes that code for the structural components of the ESX-1 secretion system [14], genes that code for accessory protein [15]and genes that code for ESX-1 substrates, including EsxA, EsxB (also known as CFP-10), PPE68, EspE, EspF, EspK and EspB (reviewed in [16, 17]). Two of the exceptions are EspA and EspC [18, 19], which are both part of the *espA* operon, which is located elsewhere in the genome. However, these genes are homologous to the *espE* and *espF* genes, respectively, which belong to the *esx-1* locus. A peculiar characteristic of ESX-1 substrates is that these substrates are mutually dependent, *i.e.*, the secretion of each of these substrates is dependent on the secretion of the other substrates [18]. The secreted ESX proteins contain a conserved WxG amino acid motif located between two α-helices [20]. In addition, these substrates also contain a conserved secretion signal, present in all secreted protein pairs [21]. This C-terminal YxxxD/E motif that is immediately following the helix-turn-helix domain is targeting these proteins for secretion, but does not determine the specificity for a particular type VII system [22]. Therefore, it remains difficult to bioinformatically predict ESX-1 substrates.

To establish successful infection, mycobacteria need regulatory mechanisms to express the right proteins at the right time. In different environments, mycobacteria require specific transcriptional responses to successfully respond to the stress conditions encountered. During the first stages of infection, ESX-1-mediated protein secretion is one of the most important virulence mechanisms of pathogenic mycobacteria [16, 17]. Consequently, tight transcriptional regulation of *esx-1* and the associated genes is required. The transcriptional regulator PhoP of the two-component system PhoPR positively regulates the transcription of many *esx-1*-associated genes, including genes in the *espA* operon [23–25]. It has been proposed that PhoP regulation is dependent on environmental pH [26], which could indicate that the acidic environment of the

phagosome induces *esx-1* gene transcription via PhoP, leading to bacterial escape from this compartment. Other studies have shown that the *espA* operon is, in addition to PhoP, also regulated by the transcription factors EspR and MprAB and the repressors CRP and Lsr2, indicating that tight regulation of this operon is essential and, furthermore, suggesting that the *espA* operon may be regulated in a manner distinct from the regulation of other ESX-1 substrates [27–30].

Here, we apply RNA-seq and quantitative proteomics to determine the gene expression and proteomic profiles of the pathogenic mycobacteria *M. marinum* and *M. tuberculosis* in the absence of a functional ESX-1 secretion system. During short-term infection of macrophages, we observed highly increased transcript levels of the *espA* operon. In contrast, during in vitro growth in culture medium, transcription of most ESX-1 substrates and some putative new substrates was seen to be decreased. Among the putative regulatory protein that was down-regulated in *esx-1* mutant strains of both *M. marinum* and *M. tuberculosis*, we confirmed a regulatory role for the putative transcriptional regulator WhiB6 in the gene expression of ESX-1 substrates.

Materials and methods

Bacterial strains and growth conditions

We used strain M. marinum E11 for our experiments [31, 32]. The *esx-1* mutants of the *M. marinum* E11 wild-type strain used in this study contain transposon insertions in *eccB₁*, *eccCa₁*, *eccCb₁*, *eccD₁* and *eccE₁* and have been described previously ([33]; Stoop et al, doctoral thesis 2013, "*Mycobacterium marinum* zebrafish embryo screen identifies polyphosphate kinase 1 (Ppk 1) as an important factor for virulence and granuloma formation"). The whiB6 mutant was created in the *M. marinum* M strain, which is more amenable to genetic manipulation. As parent strain we used the WT MUSA strain and the spontaneous *eccCb1* mutant Mvu [34, 35]. The *whiB6* mutant was created using the phage method described by Bardarov S [36] and the primers WhiB6 KO listed in S8 Table to produce the whiB6 flanking regions. Mutants were checked using PCR and sequencing of the amplified fragments. For *M. tuberculosis*, the attenuated double-deletion strains mc²6020 and mc²6030 of H37Rv were used, with deletions of *lysA* and *panCD* and of *RD1* and *panCD*, respectively [37, 38]. Bacterial strains were grown with shaking at 30°C (*M. marinum)* or 37°C (*M. tuberculosis*) in Middlebrook 7H9 culture medium supplemented with 10% ADC (albumin-dextrose-catalase, BD Biosciences) and 0.05% Tween-80. Culture medium containing the auxotrophic *M. tuberculosis* deletion strains was supplemented with 50 μg/ml pantothenic acid and, for mc²6020, 100 μg/ml L-lysine.

Infection of human macrophages

THP-1 monocytes were cultured at 37°C in 5% CO_2 in RPMI-1640 with GlutaMAX-1 (Gibco) supplemented with 10% FBS, 100 μg/ml streptomycin and 100 U/ml penicillin. Cells were seeded at a density of 3×10^7 cells per T175 flask and differentiated into macrophages by 48 hours of incubation with 25 ng/ml PMA (Sigma-Aldrich). Then, 1.8×10^8 THP-1 cells were infected with *M. marinum* at a multiplicity of infection (MOI) of 20 for 2 hours, after which the cells were washed with PBS to remove extracellular bacteria. After 4 additional hours of infection at 33°C, the THP-1 cells were lysed with 1% Triton X-100. After a low-speed centrifugation step to remove cellular debris, mycobacteria were pelleted, after which RNA was extracted as described in the following section.

Genome sequence

We sequenced the *M. marinum* E11 strain with PacBio RSII single-molecule real-time (SMRT) sequencing technology [39]. The raw reads were assembled into two pieces (the core

and the plasmid) with HGAP assembler [40] using the default parameters. The sequence was improved with iCORN2 [41] with three iterations, correcting 20 single base pair errors and 61 insertions and deletions. To transfer the annotation from the current reference, we used RATT [42] with the PacBio parameter. Gene models around gaps were manually improved on the new sequence. The updated genome annotation was resubmitted under the same accession numbers (HG917972 for the *M. marinum E11* main chromosome genome and HG917973 for the *M. marinum E11* pRAW plasmid; complete sequences).

RNA extraction and qRT-PCR

M. marinum and *M. tuberculosis* cultures were pelleted and bead beated in 1 ml of TRIzol (Invitrogen) with 0.1-mm zirconia/silica beads (BioSpec Products). After centrifugation, supernatants were extracted with chloroform, and RNA was precipitated with isopropanol. RNA pellets were washed with 80% ethanol and dissolved in RNAse-free water. Contaminant DNA was removed by incubation with DNAse I (Fermentas). For RT-PCR, cDNA was generated using a SuperScript VILO cDNA Synthesis Kit (Invitrogen). An equivalent of 5 ng of RNA was used in the quantitative PCRs. qRT-PCR was performed using SYBR GreenER (Invitrogen) and a LightCycler 480 (Roche) instrument. Transcript levels were normalized to the levels of the housekeeping gene *sigA* [43] using ΔΔCt analysis. All primer sequences used for qRT-PCR are listed in S8 Table.

RNA preparation for Illumina sequencing

Total RNA was extracted with TRIzol (Invitrogen) and then purified on RNeasy spin columns (Qiagen) according to the manufacturer's instructions. RNA integrity (RNA integrity score≥6.8) and quantity were determined on an Agilent 2100 Bioanalyzer (Agilent; Palo Alto, CA, USA). As ribosomal RNA constitutes a vast majority of the extracted RNA population, depletion of these molecules via RiboMinus-based rRNA depletion was conducted. For mRNA enrichment, Invitrogen's RiboMinus Transcriptome Isolation Kit, bacteria was used according to manufacturer's instructions. Briefly, 2μg of total RNA samples was hybridized with prokaryotic rRNA-sequence-specific 5′-biotin-labelled oligonucleotide probes to selectively deplete large rRNA molecules from total RNA. Then, these rRNA-hybridized, biotinylated probes were removed from the sample with streptavidin-coated magnetic beads. The resulting RNA sample was concentrated using the RiboMinus concentrate module according to the manufacturer's protocol. The final RiboMinus RNA sample was subjected to thermal mRNA fragmentation using the Elute, Prime, Fragment Mix from the Illumina TruSeq RNA Sample Preparation Kit v2 (Low-Throughput protocol). The fragmented mRNA samples were subjected to cDNA synthesis using the Illumina TruSeq RNA Sample Preparation Kit (low-throughput protocol) according to the manufacturer's protocol. Briefly, cDNA was synthesized from enriched and fragmented RNA using SuperScript III reverse transcriptase (Invitrogen) and the SRA RT primer (Illumina). The cDNA was further converted into double-stranded DNA using the reagents supplied in the kit, and the resulting dsDNA was used for library preparation. To this end, cDNA fragments were end-repaired and phosphorylated, followed by adenylation of 3′ ends and adapter ligation. Twelve cycles of PCR amplification were then performed, and the library was finally purified with AMPure beads (Beckman Coulter) as per the manufacturer's instructions. A small aliquot (1 μl) was analysed on an Invitrogen Qubit and an Agilent Bioanalyzer. The bar-coded cDNA libraries were pooled at equal concentrations before sequencing on an Illumina HiSeq2000 using the TruSeq SR Cluster Generation Kit v3 and TruSeq SBS Kit v3. Data were processed with Illumina Pipeline software v1.82.

RNA-seq analysis

The Illumina reads were mapped with SMALT (http://www.sanger.ac.uk/science/tools/smalt-0) (default parameters) against the new PacBio reference. From the read count, which was obtained with bedtools ([44], parameter multicov, with -D to include duplicates and -q 5 to exclude repetitive mapping reads), we performed a differential expression analysis with DESeq [45] using default parameters.

Plasmid construction

The *E. coli*-mycobacterial shuttle vector pSMT3 was used for the construction of all plasmids. To overexpress PE35-PPE68_1 (MMARE11_01740- MMARE11_01750), we used a previously described plasmid [22]. For construction of the plasmid containing *espG$_1$*, this gene was amplified from the *M. marinum* E11 genome by PCR using primers containing NheI and EcoRV restriction sites and a 3' HA epitope. The resulting PCR product and empty pSMT3 were digested with NheI and EcoRV followed by ligation of *espG$_1$* into the vector by T4 ligase (Fermentas). For construction of the plasmid containing *whib6*, this gene was amplified from the *M. marinum* E11 genome by PCR using primers containing NheI and BamHI restriction sites. For the other construct, *espI* was amplified from the *M. marinum* E11 genome by PCR using primers containing NheI and BglII restriction sites. The PCR product was digested with NheI and BamHI. Empty pSMT3 was digested with NheI and BamHI, after which the PCR product was ligated into the vector. All plasmids were introduced into the *M. marinum* wild-type E11 and isogenic *eccCb$_1$* mutant strains by electroporation. All primer sequences are listed in S8 Table.

Analysis of protein expression and secretion

M. marinum cultures were grown to mid-logarithmic phase in 7H9 culture medium supplemented with 0.2% glycerol and 0.2% dextrose. Bacteria were pelleted, washed in PBS and incubated in 0.5% Genapol X-080 (Sigma-Aldrich) for 30 minutes to extract cell wall proteins. Genapol X-080-treated *M. marinum* cells were disrupted by sonication. Secreted proteins were precipitated from the culture supernatant by 10% trichloroacetic acid (TCA, Sigma-Aldrich). Proteins were separated according to molecular weight on 15% SDS-PAGE gels and subsequently transferred to nitrocellulose membranes (Amersham Hybond ECL, GE Healthcare Life Sciences). Immunostaining was performed with mouse monoclonal antibodies directed against the HA epitope (HA.11, Covance), EsxA (Hyb76-8), or rabbit polyclonal sera recognizing EspE [46].

LC-MS analysis

Peptide preparation from the *M. marinum* E11 and isogenic *eccCb1* mutant strains was performed as previously described [47]. Approximately 100-µg protein digests of each sample were labelled with 4plex iTRAQ reagents (Applied Biosystems). The combined iTRAQ-labelled samples were fractionated using strong cation exchange chromatography. The eluted fractions were dried and desalted using a Sep-Pak C-18 SPE cartridge (Waters, Milford, MA, USA). LC-MS analysis as well as MS data processing was carried out following our published procedure [48]. Briefly, each fraction was analysed three times using an LTQ-Orbitrap Velos (Thermo Scientific). The MS spectra were recorded in the Orbitrap, whereas the MS2 spectra were recorded in the c-TRAP for HCD fragmentation and in the LTQ for the CID fragmentation. Both HCD and CID spectra were extracted separately using Proteome Discoverer software and processed by an in-house script before a Mascot search against the *M. marinum* E11

proteome. The Mascot results (.dat file) were processed by Scaffold software for validation of protein identification and quantitative assessment. For protein identification, local false positive rates (FDR) were maintained below 1% for both protein and peptide identification (0.91% and 0.9% for peptides and proteins, respectively, for this dataset). Protein quantitation was processed using Scaffold Q+, which is based on the i-Tracker algorithm [49]. The iTRAQ quantitation using HCD is highly accurate, and a change of more than 2-fold was considered significant differential expression in this study.

Results

Global features of the *M. marinum eccCb1* mutant transcriptome and proteome

To investigate the effect of ESX-1 disruption on gene expression and protein production, RNA and protein were extracted from three independent exponential phase cultures of the *M. marinum* E11 strain and the isogenic *esx-1*-mutant during growth in 7H9 culture medium to characterize the transcriptome and proteome. Using transcriptomics (RNA-seq) and mass spectrometry (MS)-based proteomics with isobaric labelling for quantification, we captured the expression dynamics of the transcripts and proteomes of the *eccCb1* mutant. Data quality was assessed using Euclidean distance matrices for RNA (S1 Fig) and principal component analysis (PCA) for protein (S2 Fig), which demonstrated high levels of reproducibility between biological replicates. After filtering (see Materials and Methods for details), a total of 823 genes were identified as being differentially expressed (DE) as messenger RNA, of which 525 were classified as down-regulated and 298 as up-regulated (Fig 1A and S1 Table). To determine parallel changes in protein levels, 1,657 proteins were identified by the presence of 2 or more peptides, of which 576 proteins passed our filter and we classified them as DE. Of these, 412 proteins were found to be down-regulated and 164 were up-regulated (S2 Table), and 482 protein-coding genes were shared and were identified in both the RNA-seq and quantitative proteomic datasets (Fig 1C).

The degree of global correlation between the gene expression and protein abundance scores among the shared genes was relatively low (S3A Fig), which has also been noted in other bacterial studies [50]. However, within certain classes of *M. marinum* functional categories (http://mycobrowser.epfl.ch/marinolist.html), the degree of correlation was much higher than that in other classes, with R^2 exceeding 0.8 for the categories such as lipid metabolism (Fig 1D), regulation (Fig 1E) and cell wall and cell processes (Fig 1F). Of the DE genes at the RNA and protein levels, 28% were in the intermediary metabolism and respiration category, 18% were in the cell wall and cell process category, 15% were in the information pathways category and 14% were in the lipid metabolism category (S4 Fig).

Transcriptional profiling analysis of the double auxotrophic *M. tuberculosis* mc²6020 mutant strains [38] and their isogenic *esx-1* mutants during growth was carried out to identify genes for which expression was dependent on ESX-1 disruption (Fig 1B and S3 Table). For this species, the same trends could be identified as for *M. marinum*.

Major effects of *esx-1* mutation on genes encoding ESX-1 substrates and biosynthetic pathways

Analysis of differential expression in *M. marinum* identified changes in genes involved in a variety of cellular processes (Fig 2), although a majority of the most differentially regulated genes were associated with cell wall and cell processes and lipid metabolism. We noted that a substantial number of *esx-1*-associated genes were down-regulated in the mutant strains
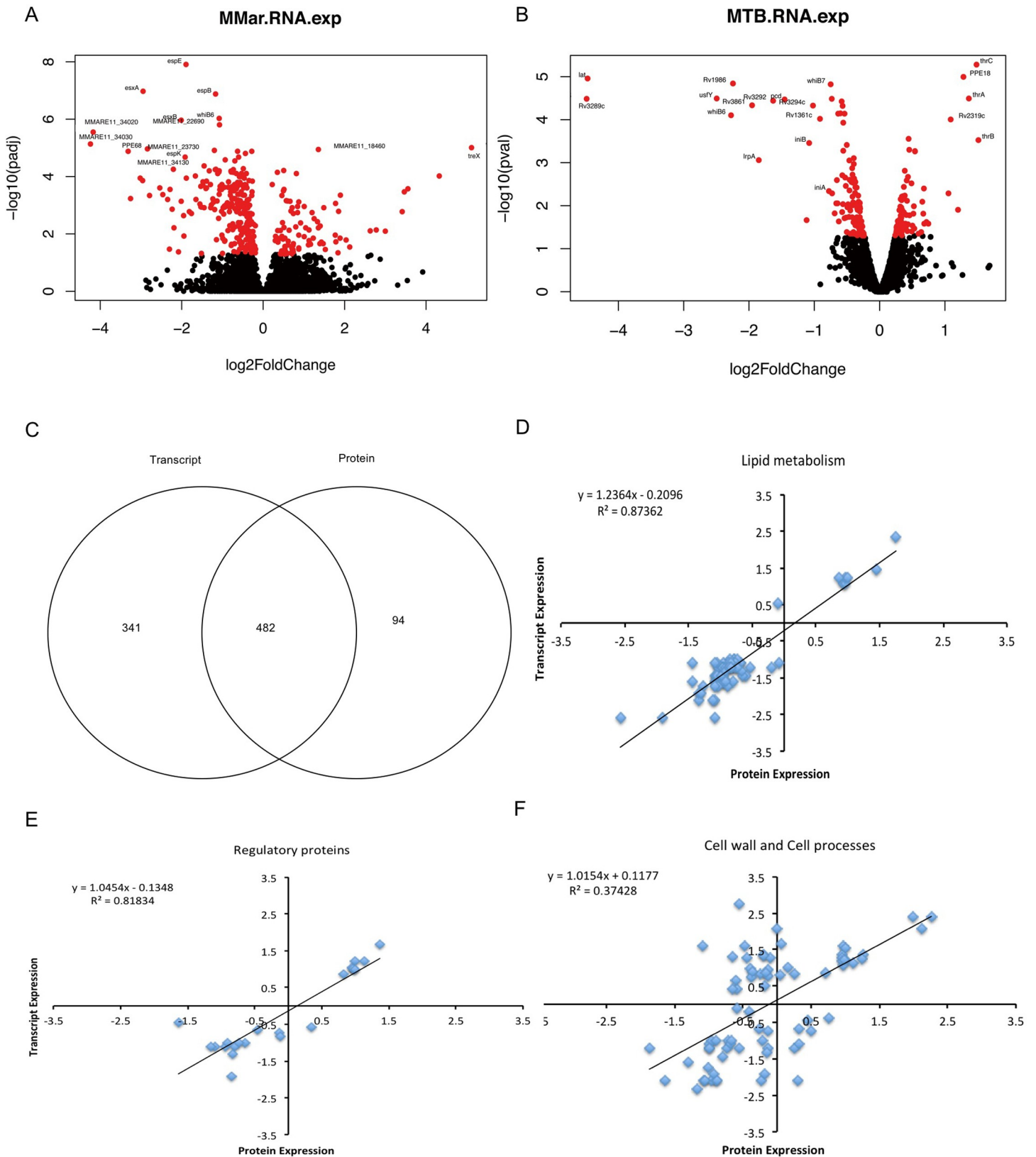
Fig 1. Global features of the transcriptomes and proteomes of the *M. marinum* and *M. tuberculosis esx-1* mutant strains. Volcano plots obtained from RNA-seq analysis of the wild-type *M. marinum* E11 strain vs. the *eccCb₁* transposon mutant (A) and of *M. tuberculosis* mc²6020 vs. the *esx-1* mutant strain (B). Each dot indicates

the expression value of a gene. Red dots indicate statistical significance ($q < 0.05$), and black dots indicate a lack of statistical significance. Selected genes that are most down- or up-regulated in the *esx-1* mutant strains are highlighted. (C) Venn diagram of the number of differentially expressed transcripts and proteins quantified of *M. marinum eccCb₁* mutant using RNA-seq and quantitative proteomics, respectively. Scatterplots of the relationship between differentially expressed genes of *M. marinum eccCb₁* transposon mutant and those of the isogenic wild-type strain E11, quantified in both data sets and classified into the following categories: (D) lipid metabolism, (E) regulatory proteins and (F) cell wall and cell process. Scatterplots and bar chart show the rectilinear equation and the Pearson correlation coefficient (R^2).

https://doi.org/10.1371/journal.pone.0211003.g001

during growth in culture medium, including 11 genes that were located within or directly adjacent to the *esx-1* gene cluster. Among these down-regulated genes were those coding for known ESX-1 substrates, such as EsxA, EsxB, EspE and EspB. Remarkably, mRNA levels of core components of the ESX-1 secretion system, *i.e.*, those encoding members of the type VII secretion complex, such as $EccB_1$, $EccD_1$, $EccE_1$ and $MycP_1$, remained unchanged, even though the corresponding genes are interspersed with genes encoding ESX-1 substrates. In contrast to the mRNA levels, we noted a strong increase in the protein levels of EsxA and EsxB, probably reflecting the accumulation of these proteins in the cell due to the secretion defect (Fig 2). Our data also indicate a significant effect of *esx-1* disruption on genes associated with lipid metabolism (Fig 2), including genes associated with the synthesis of mycolic acids. Strong down-regulation was observed at the mRNA and protein levels for several polyketide synthases, including genes involved in mycolic acid biosynthesis, such as *umaA*, *mmaA3*, *accD5*, *accD6*, and *pks15/1*, which encode components of the lipid biosynthesis pathway (Fig 2 and S1 and S2 Tables). The changes observed in *esx-1* and lipid-metabolism-associated genes at the mRNA and protein levels were not unexpected; it has been reported previously that ESX-1-dependent protein secretion and mycolic acid synthesis are critically linked [51]. However, we also noted a surprisingly broad impact of ESX-1 mutation on major biosynthetic pathways, including ribosomal protein synthesis and DNA biosynthesis (S1 and S2 Tables). Down-regulation was observed at the mRNA and protein levels for several genes encoding ribosomal proteins and DNA gyrase and a ribonucleotide-diphosphate reductase, which are components of protein and DNA biosynthesis, respectively. We also identified changes at both the mRNA and protein levels in genes involved in general stress response (*grpE*, *dnaK*, *groES*, *groEL1*), genes involved in stress response regulation (*sigA*, *sigB*, *devS*), members of the WhiB family (*whiB2*, *whiB4*, *whiB6*) and several PE_PGRS genes (Fig 2). The *M. tuberculosis esx-1* mutation did not seem to have a significant effect on the expression of genes involved in lipid metabolism compared to the effect seen in *M. marinum* (Fig 2 and S1 and S3 Tables). Finally, a significant number of genes that are associated with information pathways, including genes encoding ribosomal proteins, were up-regulated at the mRNA level in the *eccCb* mutant (Fig 2). Taken together, the observed changes in the transcriptome and proteome of mutants defective in ESX-1 secretion reflect the role this cluster employs for major biochemical pathways in *M. marinum* and *M. tuberculosis*.

Global transcriptional profiling of intraphagosomal *M. marinum* and the *eccCb1* mutant

We next determined the effect of ESX-1 abrogation in *M. marinum* on gene transcription during infection of primary macrophages. Using a PMA-differentiated THP-1 cell line as a model of primary macrophages, we analysed the global gene expression of the wild-type and *eccCb1* mutant strains of *M. marinum* after 6 hours of infection. Wild-type mycobacteria can escape the phagosome within two hours after infection [52], whereas ESX-1 secretion mutants of both *M. marinum* and *M. tuberculosis* are known to be limited to the phagosomal compartment [53]. The intraphagosomal transcriptome of the *eccCb1* mutant was compared with the intracellular transcriptome of wild-type *M. marinum*. Furthermore, these intracellular
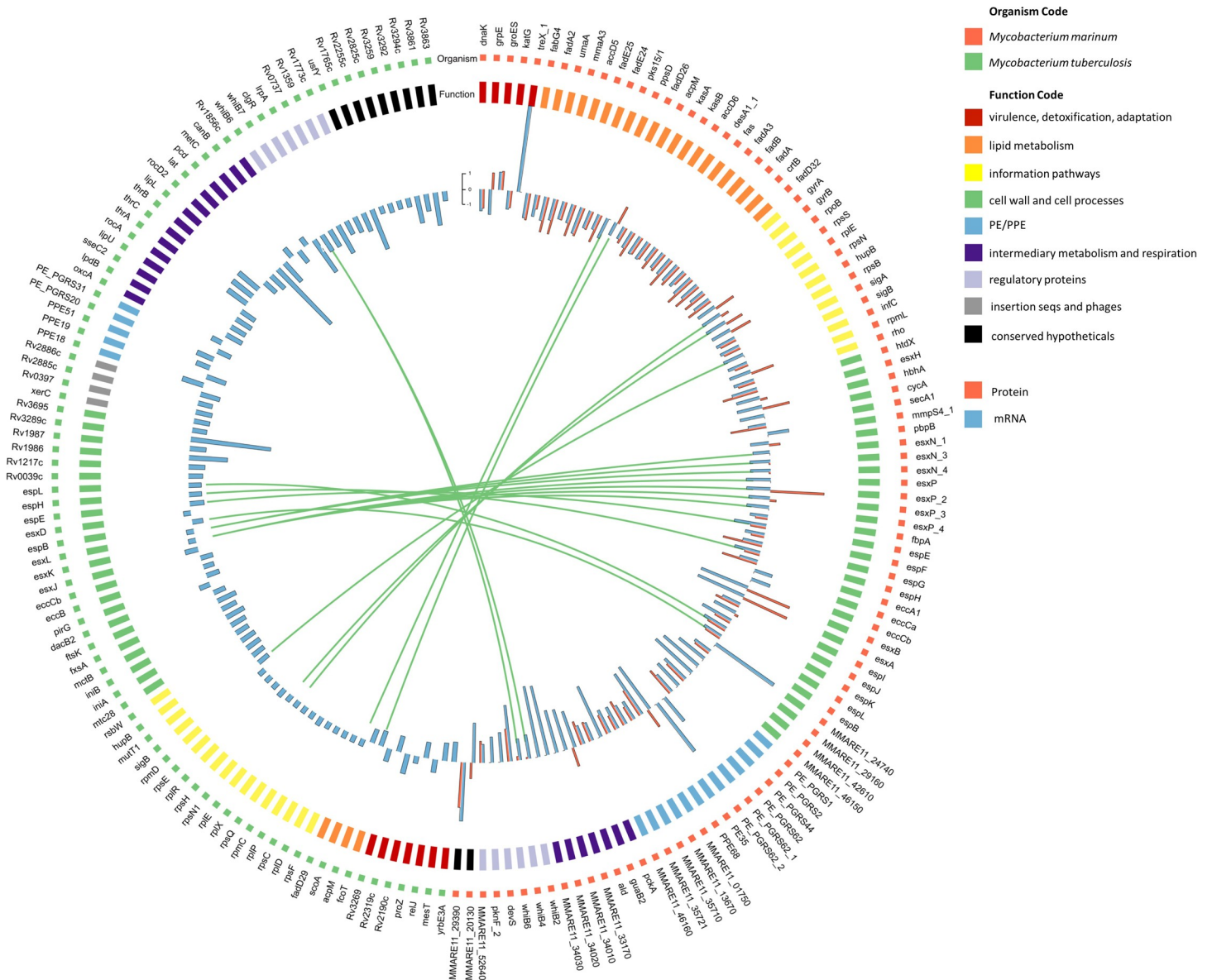
Fig 2. Top differentially expressed genes of *M. marinum* and *M. tuberculosis*, when grown in culture medium, grouped into broad functional categories. Within each group, genes are ranked in ascending order by *p*-value. (Red) Top 100 annotated *M. marinum* E11 genes that exhibit greatest differential expression in the *M. marinum eccCb₁* transposon mutant compared to the isogenic wild-type strain E11 during growth in 7H9 culture medium. Bar chart of log2-fold change for individual genes (RNA, blue; protein, red; locus tags, outer). (Green) Top 100 annotated *M. tuberculosis* genes that exhibit greatest differential expression in the auxotrophic *M. tuberculosis* RD1 deletion mutant strain mc²6030 compared to the isogenic control strain mc²6020 during growth in 7H9 culture medium. Bar chart of log2-fold change for individual genes. The genes *rv3872-rv3878* are not included as these genes are deleted in the RD1 mutant strain.

transcriptomes were also compared with the transcriptome of wild-type *M. marinum* grown in standard broth culture. We identified 720 (p<0.05) genes in the *eccCb1* mutant that exhibited significant changes in expression after THP-1 infection compared to the expression levels in the wild-type strain. Of these genes, 465 were down-regulated and 255 were up-regulated (S4 Table and S5 Fig). Remarkably, none of the genes within the *esx-1* region were significantly differentially expressed in the *esx-1*-mutant compared to the wild-type strain. However, we found a specific and pronounced increase in the transcript levels of the *espA* operon in the

intraphagosomal transcriptome of the *eccCb1* mutant as compared with the levels in the *in vitro* transcriptomes (Fig 3A). During growth in culture medium, the mRNA levels of *espA* did not differ between the wild-type and *esx-1*-deficient *M. marinum* strains, which was confirmed by quantitative RT-PCR (qRT-PCR) (Fig 3B). Therefore, these data suggest that proteins encoded by the *espA* operon, *i.e.*, EspA, EspC and EspD, may play an important role in ESX-1-specific processes during the first stages of macrophage infection. The *espA* operon was also induced in the wild-type bacteria inside macrophages, albeit at a lower level. Perhaps this difference exists because the wild-type bacteria are able to escape from the phagosome, whereas the *eccCb1* mutants are not.

Further analysis showed that a significant number of genes that code for proteins involved in cell wall and cell processes were differentially regulated by intracellular wild-type *M. marinum* and the ESX-1-deficient strain in comparison with their counterparts grown in culture medium (S5 and S6 Tables). *M. marinum* genes involved in mycolic acid synthesis, phthiocerol dimycocerosate (PDIM) synthesis and transport to the cell surface, such as *fabG1*, *accDs*, *ppsC*, *ppsD*, *pks11_1*, *pks13*, as well as genes coding for polyketide synthases and the mycolic acid methyltransferase *umaA* were differentially expressed during infection of THP-1 cells (Fig 3C and 3D). Furthermore, *cpsY*, a gene that encodes UDP-glucose 4-epimerases and is essential for linking peptidoglycans and mycolic acid [54], exhibited a pronounced increase in mRNA level in the intracellular *eccCb1* mutant (S4–S7 Tables). We also found that many genes associated with cell division and peptidoglycan assembly, such as *ftsE*, *ftsH*, *ftsW*, *murC*, and *murG* [55, 56], were down-regulated by intracellular bacteria (S4–S7 Tables).

A significant number of genes that code for proteins associated with lipid metabolism and metabolic adaptation were differentially regulated in macrophages (S6A Fig). This subset includes genes involved in fatty acid metabolism such as isocitrate lyase (*icl*), an enzyme necessary for the glyoxylate cycle and required for intracellular survival [57, 58], and *pckA*, which encodes the phosphoenolpyruvate carboxykinase and is essential for mycobacterial survival in both macrophages and mice [59, 60] and is involved in energy metabolism (S6B Fig), and the KstR-dependent cholesterol regulon (S6C Fig), which is involved in lipid degradation and carbon metabolism [61]. We also observed effects of a number of genes involved in general stress response (*groES*, *groEL1*, *hsp*, *ahp*, *dnaK*), genes involved in stress response regulation (*sigB*, *devR*, *devS*, *hspR*, *kstR*), members of the WhiB family (*whiB2*, *whiB3*, *whiB4*, *whiB*, *whiB6*, *whiB7*) and alternative sigma factors (*sigE*, *sigL*, *sigM*) in the *eccCb1* mutant during infection to macrophages. This pattern is illustrated in S6D Fig and is probably associated with stressful intraphagosomal conditions.

Different *M. marinum esx-1* transposon mutants have similar gene transcription profiles

The ESX-1-deficient strain of *M. marinum* used for RNA sequencing contains a transposon in the *eccCb1* gene. To confirm that the observed gene transcription effects were due to a defective ESX-1 system and not due to a side effect of this particular mutation, we analysed several mutants containing transposon insertions in different genes from the *esx-1* gene cluster and compared the mRNA levels of the selected genes by qRT-PCR. Our results showed decreased transcript levels of the known ESX-1 substrate *esxA* and other *esx-1* secretion-associated (*esp*) genes, namely, *espL*, *espK* and *espJ*, for all tested *eccCb1* mutants, whereas the transcript levels of *eccD1*, which encodes a structural component of the ESX-1 system [14], did not differ from the transcript levels in wild-type *M. marinum* (Fig 4). These gene expression patterns in the *eccB1*, *eccCa1*, *eccD1* and *eccE1* transposon mutants were similar to the RNA sequencing results obtained for the *eccCb1* mutant. The only exception was that for the mutant containing a
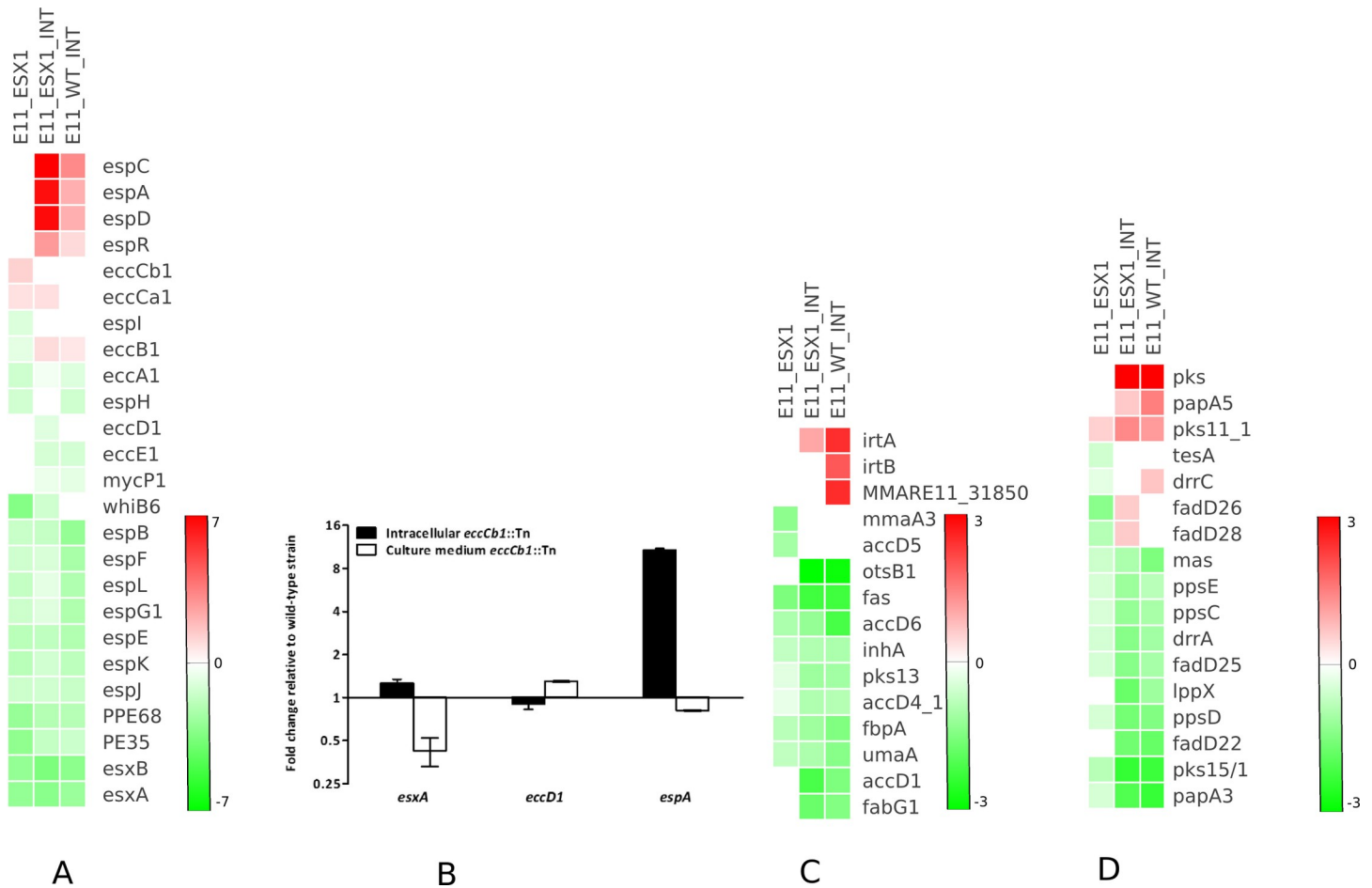
Fig 3. Effect of ESX-1 disruption (*M. marinum eccCb1* Transposon Mutant) on gene transcription during infection (Indicated as ínt') and growth in culture medium in *M. marinum* compared to that in the wild-yype strain E11 during growth in 7H9 culture medium. (A) Relative transcript expression levels of the ESX-1 secretion system-associated genes, including the main *esx-1* locus as well as the EspR regulator and accessory factors in the *espA* operon, which is encoded outside the RD-1 region. (B) Gene expression levels, as measured by qRT-PCR, were compared to those of the wild-type strain E11 grown in similar conditions. Values represent mean ± standard error of the mean of two biological replicates. (C, D) Regulation of genes associated with cell wall synthesis, including genes involved in mycolic acid synthesis (C) and PDIMs (D).

transposon insertion in *eccD₁*, we observed an increase of *eccD₁* transcription itself and, to a lesser extent, an increase of the adjacent gene *espJ* (Fig 4). However, this increase was most likely due to the presence of a strong promoter on the transposon, driving the transcription of the kanamycin resistance cassette, as the measured mRNA is transcribed from sequences directly downstream of this promoter. Altogether, our results demonstrate that inactivation of the ESX-1 secretion system leads to down-regulation of the transcription of ESX-1 substrates and associated proteins.

ESX-1 substrate gene transcription is reduced by a regulatory mechanism

We next sought to determine the molecular mechanism underlying the down-regulation of specific transcripts in *eccCb1* mutant strains of *M. marinum*. It is possible that the decrease in mRNA levels is due to a regulatory effect at the transcriptional level. Alternatively, the down-regulated mRNA may be degraded via a post-transcriptional mechanism. To investigate these possibilities, we expressed an extra copy of the *espL* gene under the control of a constitutively
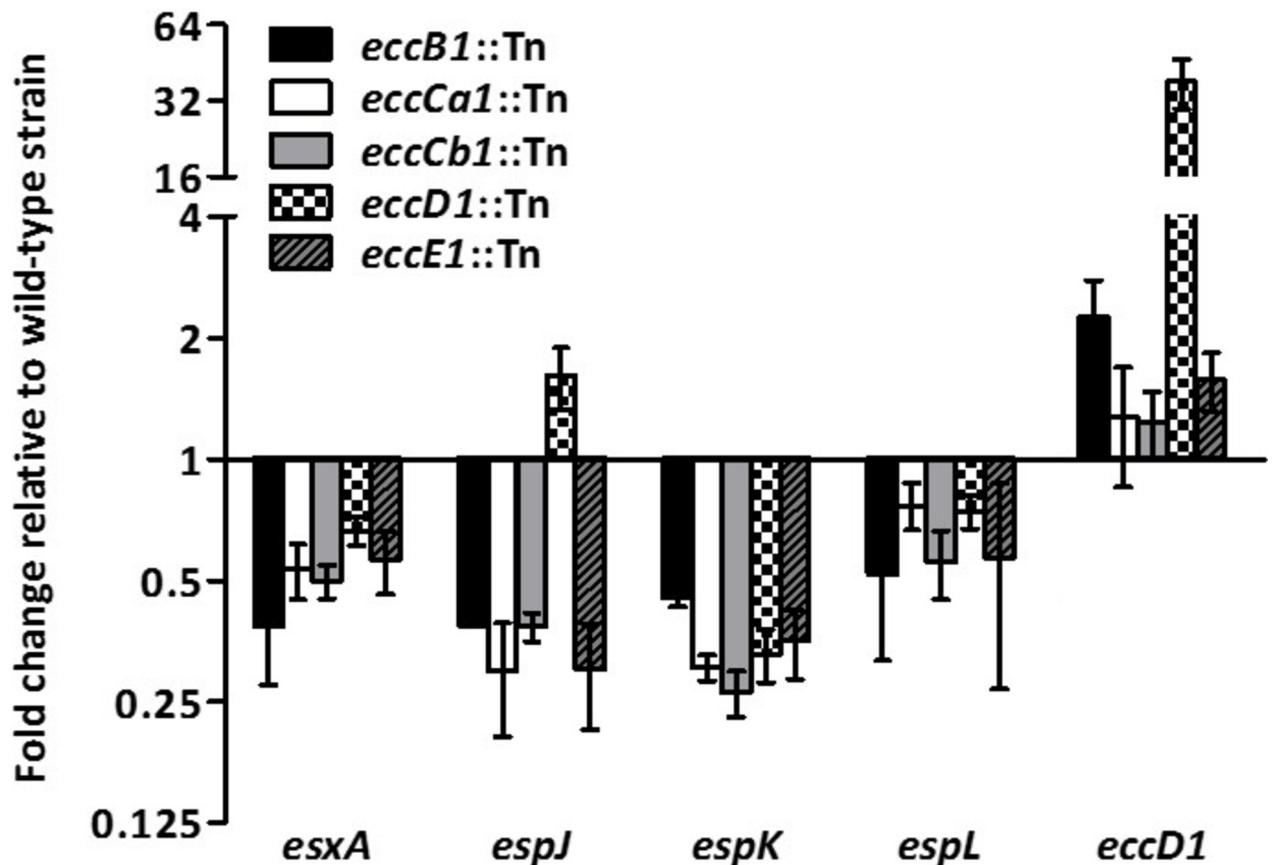
Fig 4. *Esx-1* transposon mutants have similar gene transcription profiles. Gene expression levels for *M. marinum eccB_1*, *eccCa_1*, *eccCb_1*, *eccD_1* and *eccE_1* transposon mutants as measured by qRT-PCR. All strains were grown in 7H9 culture medium, and gene expression levels were compared to those of the wild-type strain E11. Values represent mean ± standard error of the mean of at least three biological replicates.

active promoter in the wild-type and *eccCb_1* mutant strains of *M. marinum* and determined the *espL* gene transcript levels. We found a similar increase in *espL* transcripts in both the wild-type and *eccCb_1* mutant strains, indicating that degradation of specific mRNA is probably not the cause of the decreased mRNA levels in the mutant strain (Fig 5A). Expression levels of the downstream gene *espK* were not affected by the introduction of *espL*. These results indicate that there is a regulatory mechanism that prevents the transcription of genes encoding ESX-1 substrates and associated proteins in the absence of a functionally active ESX-1.

PE35 and PPE68 play an important role in ESX-1 secretion but not in gene regulation

Previously, PE35, which is located within the *esx-1* gene cluster, has been implicated to be essential for EsxA and EsxB secretion in *M. tuberculosis* [62]. In contrast to this proposed function, the PE35/PPE68_1 protein pair in *M. marinum* is secreted via ESX-1 [63, 64]. To determine whether PE35 plays a role in the regulation of ESX-1 substrates, we overexpressed the *pe35/ppe68_1* operon in *M. marinum*. Interestingly, although there was no effect on gene transcription (Fig 5C), we noticed a substantial increase in EsxA secretion in the wild-type strain (Fig 5B). This increased EsxA secretion does not seem to represent a general increase in ESX-1 secretion, as protein levels of the cell-surface-localized EspE remained similar (Fig 5B). To
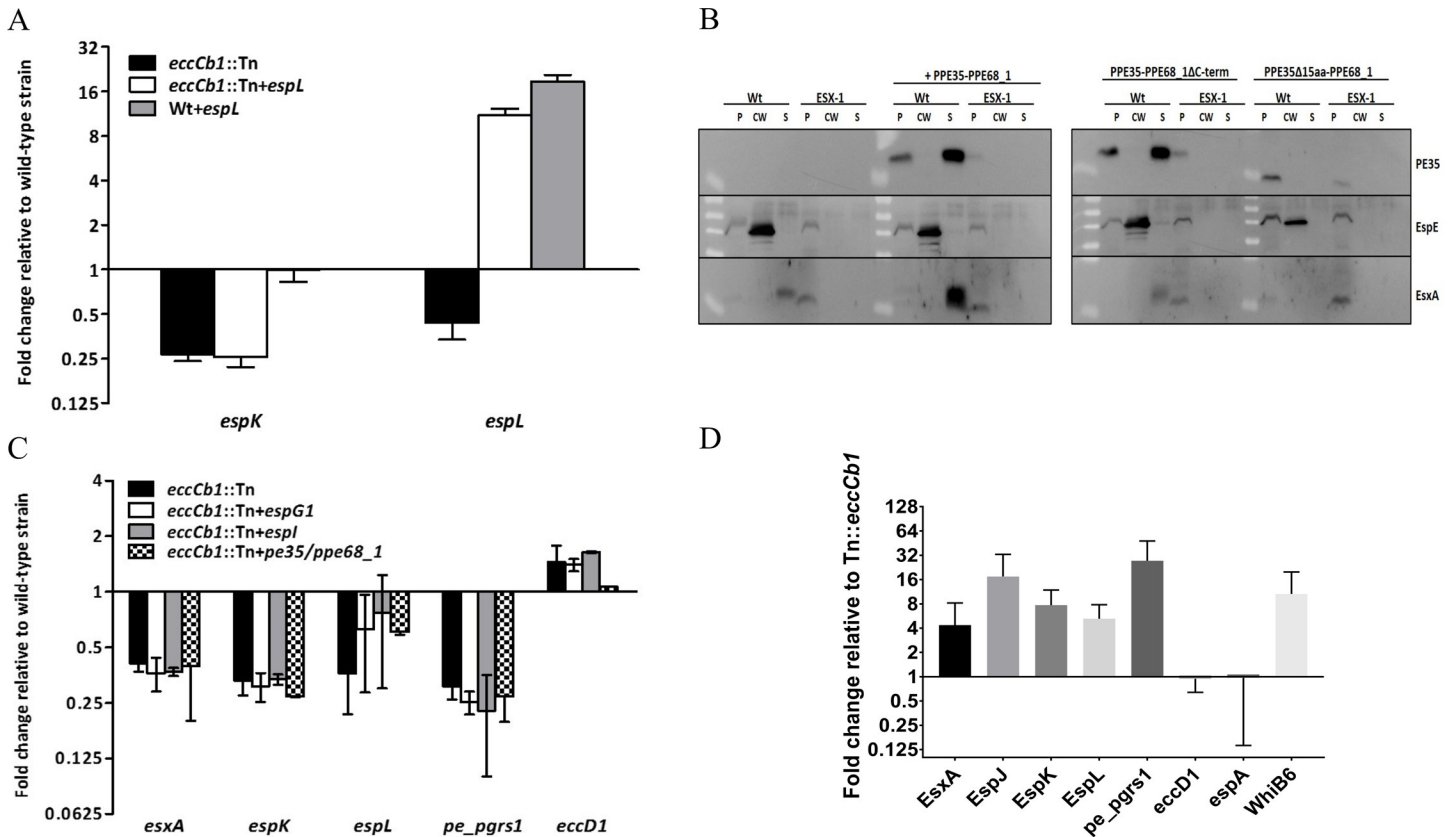
Fig 5. Regulation of the ESX-1 secretion system. (A) Down-regulation of *espL* is the result of a regulatory process. A functional copy of *espL* was introduced into wild-type and *eccCb1* mutant strains of *M. marinum*, and the espK and espL gene expression levels were measured by qRT-PCR. Gene expression levels were compared to those of the wild-type strain E11. Values represent mean ± standard error of the mean of two biological replicates. (B) Introduction of PE35/PPE68_1 result in increased EsxA secretion but not in gene regulation. Pellet (p), cell wall extract (cw), and supernatant (s) fractions of the wild-type and *eccCb1* mutant strains of *M. marinum* expressing PE35/PPE68_1; PE35/PPE68, containing a C-terminal deletion of PPE68_1; or PE35/PPE68_1, containing a 15-amino-acid C-terminal deletion of PE35, were analysed for the presence of EspE, EsxA and the introduced PE35 by immunoblotting. Fractions represent 0.5, 1 or 2 OD units of original culture. In all cases, PE35 contained a C-terminal HA tag. (C) EspG1, EspI and PE35/PPE68_1 do not regulate the transcription of selected *esx-1*-associated genes. EspG1, EspI or PE35/PPE68_1 were overexpressed in the *M. marinum* eccCb1 mutant strain, and the expression levels of *espK*, *espL*, *esxA*, *pe_pgrs1* and *eccD1* were measured by qRT-PCR. Gene expression levels were compared to those of the wild-type strain E11. Values represent mean ± standard error of the mean of at least two biological replicates. (D) WhiB6 is involved in transcriptional regulation of ESX-1 substrates and associated genes. The *whib6* gene was overexpressed in the *M. marinum eccCb1* mutant strain, and transcript levels of *espK*, *espL*, *esxA*, *pe_pgrs1* and *eccD1* were measured by qRT-PCR. Gene expression levels were compared to those of the *eccCb1* mutant strain. Values represent mean ± standard error of the mean of two biological replicates.

study this effect in more detail, we introduced PE35 with a truncated version of PPE68_1 that contained only the PPE domain and was devoid of the C-terminal portion. Although the introduced PE35 protein was expressed and secreted efficiently by ESX-1 (Fig 5B), the levels of secreted EsxA were not increased, indicating that the C-terminal portion of PPE68_1 plays a role in EsxA secretion. To determine whether secretion of the PE35/PPE68_1 protein pair itself was important for this process, we also determined the effect of removal of the last 15 amino acids of the PE protein, which contained the general secretion signal. This small deletion not only abolished the secretion of the introduced PE35 protein but also abolished EsxA secretion completely, despite the presence of an intact chromosomal copy of the *pe35/ppe68_1* operon (Fig 5B). This result suggests that the truncated form of PE35 somehow interferes with EsxA secretion. Together these data show that, although PE35 and PPE68_1 do not seem to regulate the transcription of genes encoding ESX-1 substrates, these proteins have a strong effect on EsxA, as previously observed [62].

Increasing EspI and EspG$_1$ levels does not affect *esx-1* gene expression

A second candidate protein that might regulate gene expression levels of ESX-1 substrates is EspI. The gene encoding this *esx-1*-secretion-associated protein of unknown function is located within the *esx-1* region and is down-regulated in *esx-1* mutants of both *M. marinum* and *M. tuberculosis* (Fig 2). In contrast to the other Esp proteins, EspI contains a putative nucleotide-binding domain. Previous study has shown that in *M. tuberculosis* EspI is involved in reduction of ESX-1 secretion in response to low cellular ATP levels [65]. However, when we overexpressed this protein, we did not observe a change in the down-regulation of *esx-1*-associated gene transcription in the *M. marinum eccCb$_1$* transposon mutant, suggesting that EspI does not regulate this process in our strain (Fig 5C). We next focused on EspG$_1$ as a candidate *esx-1* gene regulator. EspG$_1$, interacts specifically with PE35/PPE68_1 in *M. marinum* [63] and might function as a sensor that measures protein levels of intracellular ESX-1 substrates. To investigate the effect of EspG$_1$ on *esx-1*-associated gene expression and protein levels, we increased EspG$_1$ levels by overexpressing the *espG$_1$* gene in wild-type and ESX-1-deficient *M. marinum*. This overexpression did not result in altered gene transcription (Fig 5C) or ESX-1 protein secretion. Together, our data show that EspI and EspG$_1$ do not appear to play key roles in *esx-1*-associated gene regulation.

WhiB6 plays a role in the transcription of ESX-1 substrates

In addition to *espI*, another gene encoding a putative regulatory protein was down-regulated in *esx-1* mutant strains of both *M. marinum* and *M. tuberculosis*, namely, *whiB6* (Fig 2). WhiB proteins are actinobacteria-specific regulators that contain iron-sulfur clusters and are thought to act as redox-sensing transcription factors that can cause both gene activation and repression [66]. WhiB6 was suggested to be involved in the regulation of EsxA secretion [67], and subsequent studies have confirmed this suggestion [68–70]. To determine whether Whib6 has an effect on the expression levels of *esx-1* associated genes, we overexpressed this protein in the ESX-1-deficient *M. marinum eccCb$_1$* transposon mutant strain. We found that particularly those genes that were down-regulated in the mutant strain, such as *esxA* and *espK*, showed an increased secretion when *whib6* levels were increased (Fig 5D). Furthermore, expression of *eccD1* was unaltered by *whib6* overexpression, indicating that *whib6* is involved in the transcription of ESX-1 substrates and associated genes but not of the components of the ESX-1 system. Surprisingly, *whiB6* itself is also one of the genes that is down-regulated upon abrogation of ESX-1-mediated protein secretion. Our results indicate that the presence of WhiB6 in non-secreting strains has a positive effect on transcription of genes on coding ESX-1 substrates.

WhiB6 is required for the regulation of the ESX-1 system

To further study the involvement of WhiB6 in ESX-1 regulation, we constructed a deletion mutant of *whiB6*, both in *M. marinum* WT and in the *eccCb1* mutant background (*M. marinum* M^{USA} -Δ*whiB6* and *M. marinum* M^{VU} –Δ*whiB6*). First, we analyzed the effect of this mutation on all genes, except for the genes of the *esx-1* locus. This analysis identified 34 genes (p<0.05) that were downregulated in the *eccCb1* mutant strains (Fig 6A) and therefore putatively influenced by WhiB6. Complementation of both mutants with the *whiB6* gene on a mycobacterial shuttle plasmid reversed the upregulation of these genes and generally resulted in decreased expression levels (Fig 6A and 6B). As expected, several genes that are associated with oxidative stress (*ahpC*, *ahpD*, *rebU*) were found in the differently expressed gene pool. Also, the enrichment analysis of the associated Gene Ontology terms for the differently expressed genes (*dnaB*, *dinP*) reveal that WhiB6 may also regulate DNA replication or repair through regulating DNA-directed DNA polymerase and DNA helicase (S7 Fig). Another
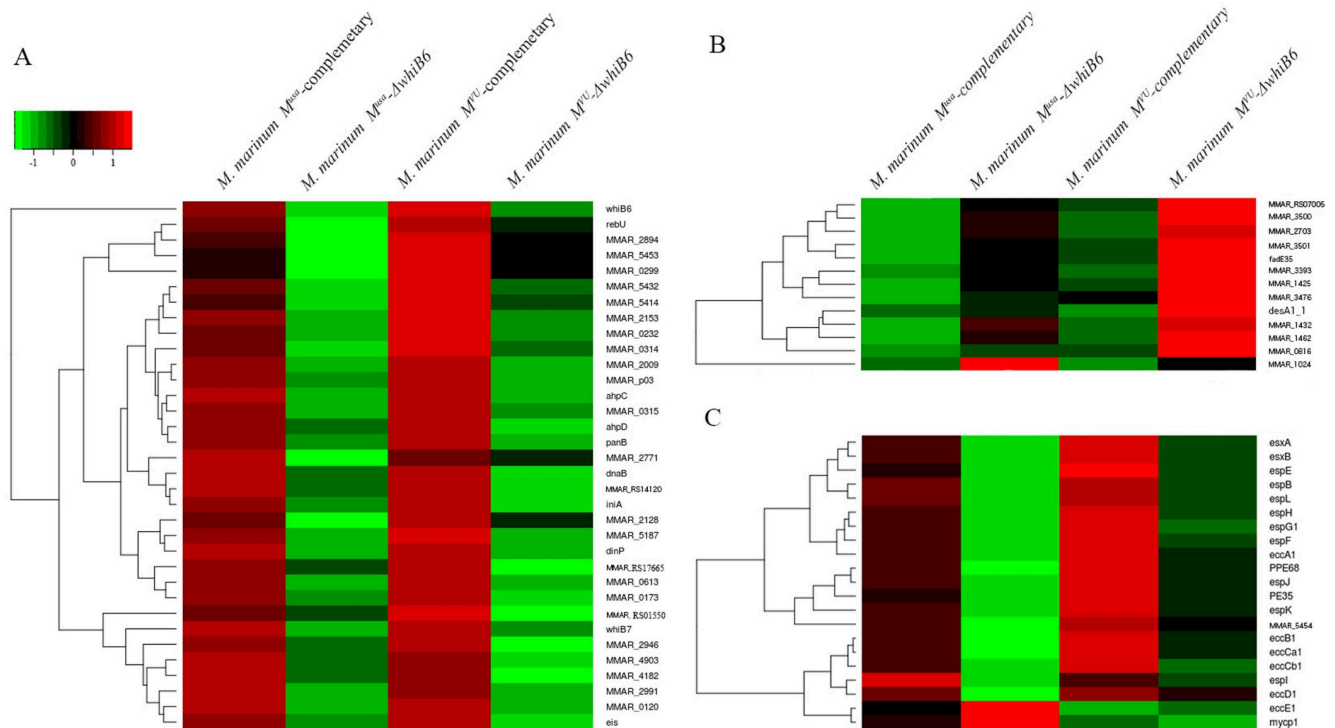
Fig 6. Gene expression profiles (Log2 Fold Change) of the complementary strains (*M. marinum* M^{USA}-complementary and *M. marinum* M^{VU}-complementary) and knock-out strains (*M. marinum* M^{USA} -ΔwhiB6 and *M. marinum* M^{VU}-ΔwhiB6) compared with those of the corresponding control strains (*M. marinum* M^{USA}-empty vector strain and *M. marinum* M^{VU}-empty vector). The red colour represents up-regulate genes and green colour represents down regulate genes compared with the control strains. The heat map of expression of the whiB6-activated gene set is shown in (A); Expression of the *esx-1* locus is shown in (B); and (C) shows the WhiB6-repressed gene set.

noteworthy gene affected by *whiB6* deletion is *iniA*, which is associated with cell wall stress induced by specific antibiotics. Interestingly, *whiB7* is within the *whiB6-active* gene set, which implies that WhiB7 is active by, or works with WhiB6. Other than the *whiB6*-active gene set, 13 genes, which are involved in iron-sulfur cluster binding, cellular lipid metabolic processes are downregulated.

Remarkably, these genes are almost exclusively downregulated in the *whiB6 esx-1* double mutant, reinforcing a functional link between WhiB6 and the ESX-1 system. However, many of the downregulated genes are encoding hypothetical proteins and hence needed to be further characterized.

Separately, we analyzed the effect of the *whiB6* deletion on all *esx-1* genes. In line with our previous results, overexpression of *whiB6* in the *eccCb1* mutant resulted in downregulation of many *esx-1* genes (Fig 6C), whereas deletion of *whiB6* did not have a strong affect in the *eccCb1* mutant background. The effect was the opposite for the mutant with a functional ESX-1 system, there the whiB6 deletion had a strong positive effect on transcription of *esx-1* genes. (Fig 6C) and also this effect could be complemented. Only the structural *eccE1* and *mycP1* genes behaved differently. There are six genes that show the same pattern of up- or down-regulation as most of the *esx-1* genes in the two different *whiB6* mutants and the complemented strains. Of these six genes, 4 encode proteins that are homologous to secreted substrates and therefore are putative ESX-1 substrates or ESX-1 chaperones, *i.e.* MMAR_2894 (PE34-like protein), MMAR0299 (PE_PGRS1), MMAR5414 ((EspA-like) and MMAR5432 (EspD-like). Recently, Phan *et al.* (15) showed using proteomics that MMAR_2894 is highly reduced in the

cell surface fractions of *M. marinum esx-1* mutants. Together, these experiments show a strong linkage between WhiB6 and the regulation of different *esx-1* genes in response to secretion activity.

Discussion

In this study, we determined the transcriptomes of the *M. marinum* E11 wild-type and the double-auxotrophic *M. tuberculosis* mc^{2}6020 mutant strains and compared these transcriptomes with those of the corresponding isogenic *esx-1* mutants. We found that during the growth of *M. marinum* in 7H9 culture medium, genes encoding ESX-1 substrates, such as EsxA and other ESX-1-associated proteins, were down-regulated in the mutant strains, whereas the transcription of genes encoding several structural components of the ESX-1 system remained unaffected. This specific decrease in transcription might function as a mechanism to avoid toxic accumulation of ESX-1 substrates. Interestingly, a similar decrease in substrate production has been shown for the ESX-5 secretion system, where the PE_PGRS substrates do not accumulate intracellularly when secretion is blocked [71, 72]. However, for these PE_PGRS substrates, regulation was shown to occur post-transcriptionally [72], implying that a different mechanism is involved.

The most prominent change in gene expression that was observed upon host cell infection by the *M. marinum eccCb1* mutant strain was the increase in transcription of the *espA* operon. The specific and pronounced transcriptional increase in the expression of this operon, and not of any other *esx-1* associated gene, indicates that transcription of the *espA* operon is regulated independently of the other substrates during infection. Previously, it has been shown that the *espA* operon is regulated by different transcription and regulation factors, including EspR, MprAB and PhoPR [28, 73, 74]. Our new finding also suggests that EspA, EspC and EspD are vital for the bacteria during the early phase of infection. Since ESX-1 has been shown to be responsible for mycobacterial escape from the phagosome, which occurs within the first few hours of infection with *M. marinum* [53], the proteins produced by the *espA* operon may play an important role in this process. Consequently, the avirulent phenotype of ESX-1-deficient mycobacteria might be partly attributable to the inability to secrete EspA and/or EspC early in infection.

To determine the mechanism via which ESX-1 substrate regulation is mediated, we overexpressed proteins that may have a regulatory function. Overexpression of the *esx-1*-encoded EspI and EspG$_1$ proteins did not have an effect on the reduced transcription of ESX-1 substrates in ESX-1-deficient *M. marinum*. The putative regulatory protein WhiB6, however, did affect the transcription of these genes. While the transcript levels of *whib6* itself were decreased in *esx-1* mutants of *M. marinum* and *M. tuberculosis*, increasing WhiB6 levels by overexpression resulted in a further decrease in transcription of the ESX-1 substrate in ESX-1-deficient *M. marinum*. This result clearly indicates that WhiB6 is involved in ESX-1-associated gene regulation, as previously suggested [70]. WhiB6 response to the block in ESX-1 function to repress the genes encode substrates while whiB6 is downregulated in esx-1 mutant which may agrees with Rachel E. Bosserman's results that whiB6 regulation of ESX-1 gene expression is controlled by a negative feedback loop. Indeed, there is accumulating evidence that WhiB proteins function as transcription factors that may play a role in survival within the host (reviewed in [75]). Recently, other groups have also presented evidence supporting a role for WhiB6 in the regulation of the transcription of *esx-1* genes [68–70].

A remarkable finding in this study was that overproduction of PE35/PPE68_1 resulted in a large increase in EsxA secretion. Previously, deletion of *M. tuberculosis* PE35 had already been shown to abolish *esxA* transcription and secretion of the corresponding gene product [62].

Here, we found that EsxA and PE35 secretion are linked, as an increase in PE35 secretion resulted in a concomitant increase in EsxA secretion. The C terminus of PPE68_1 is required for this effect, indicating that this is a specific process, which is consistent with the fact that cell-surface localization of another ESX-1 substrate, namely, EspE, is unaffected by overproduction of PE35/PPE68_1. It is possible that the PPE68 proteins serve as chaperones to escort EsxA outside the bacterium, or these proteins, may be part of the secretion apparatus, making the secretion of specific substrates highly efficient.

During *M. marinum* infection of human macrophages, we found that transcription of many *pe_pgrs* and *ppe* family genes was strongly down-regulated when ESX-1 function was abrogated. As many as 50% of all genes with decreased transcript levels in the *eccCb1* mutant strain belongs to one of these gene families (S4 Table). Notably, in the wild-type strain, transcription of the *pe_pgrs* and *ppe* genes was decreased during infection in comparison to the levels observed during growth in 7H9 medium (S5 Table). As part of an adaptive response to the macrophage environment, expression of these cell-wall-localized proteins may be down-regulated in order to evade immune recognition or to reduce cell permeability [76]. The fact that in the absence of a functional ESX-1 secretion system these genes are even further down-regulated suggests that there are functional links or shared transcriptional pathways between ESX-1 and (some of the) PE_PGRS and PPE proteins, which are generally ESX-5 substrates [34].

Taken together, our results show that transcription of the *espA* locus plays an important role in ESX-1 mediated processes during the first hours of infection. Furthermore, we established a functional link between PE35 and EsxA secretion and provided evidence of a regulatory role of WhiB6 in the transcription of ESX-1 substrates and associated genes.

Accession codes

Sequencing reads have been submitted to the EMBL-EBI European Nucleotide Archive (ENA) Sequence Read Archive (SRA) under the study accession no. PRJEB8560. The expression data have been submitted to the Gene Expression Omnibus (GEO) under the submission no. GSE124341.

Supporting information

S1 Table. Complete list of genes for which the expression levels changed significantly in the *M. marinum eccCb$_1$* transposon mutant compared to the levels in the isogenic wild-type strain E11 during growth in 7H9 culture medium. $P<0.05$.
(XLSX)

S2 Table. Complete list of proteins for which the expression levels changed in *M. marinum eccCb$_1$* transposon mutant compared to the levels in the isogenic wild-type strain E11 during growth in 7H9 culture medium. Proteins with greater than 2-fold change were considered significantly differentially expressed.
(XLSX)

S3 Table. Complete list of genes for which the expression levels changed significantly ($p<0.05$) in the auxotrophic *M. tuberculosis* RD1 deletion mutant strain mc^{2}6030 compared to the levels in the isogenic control strain mc^{2}6020 during growth in 7H9 culture medium.
(XLSX)

S4 Table. Complete list of genes for which the expression levels changed significantly ($p<0.05$) in the *M. marinum eccCb$_1$* transposon mutant strain compared to the levels in

the wild-type strain E11 during infection of human THP-1 macrophages.
(XLSX)

S5 Table. Complete list of genes for which the expression levels changed significantly ($p<0.05$) in the *M. marinum* wild-type strain during infection of macrophages compared to the levels during growth in 7H9 culture medium.
(XLSX)

S6 Table. Complete list of genes for which expression levels changed significantly ($p<0.05$) in the *M. marinum eccCb₁* transposon mutant strain during infection of macrophages compared to the levels in the wild-type strain E11 during growth in 7H9 culture medium.
(XLSX)

S7 Table. Complete list of genes for which the expression levels changed significantly ($p<0.05$) in the *M. marinum eccCb₁* transposon mutant strain during infection of macrophages compared to the levels during growth in 7H9 culture medium.
(XLSX)

S8 Table. Primers used in this study. Restriction sites are shown in bold.
(XLSX)

S1 Fig. Euclidean distance matrices of RNA-seq transcriptome data showing clustering of *M. marinum* wild-type (E11) and *eccCb₁* transposon mutant (ESX-1) strains grown in culture medium (three biological replicates) or during infection of THP-1 cells (indicated as 'int').
(PDF)

S2 Fig. Principal component analysis (PCA) of biological replicates of proteome data showing clustering of *M. marinum* wild-type (E11) and *eccCb₁* transposon mutant (ESX-1) strains. PCA mapping showed clustering of biological replicates of the E11 wild-type and *eccCb1* mutant strains.
(PDF)

S3 Fig. Correlation between protein and mRNA expression of the *M. marinum eccCb₁* transposon mutant and the isogenic wild-type strain E11 during growth in 7H9 culture medium. (A) Scatterplot of the relationship between differentially expressed genes quantified in both data sets. (B-F) Scatterplots for protein and gene transcript expression classified by functional categories. Scatterplots display the rectilinear equation and the Pearson correlation coefficient (R^2).
(PDF)

S4 Fig. Functional categories of genes that are significantly changed in the transcriptome and proteome of the *M. marinum eccCb₁* transposon mutant compared to the isogenic wild-type strain E11 during growth in 7H9 culture medium. Genes exhibiting differential expression at the RNA and protein levels were grouped according to the MarinoList classification (http://mycobrowser.epfl.ch/marinolist.html).
(PDF)

S5 Fig. Most differentially expressed genes of the *M. marinum eccCb₁* transposon mutant compared to the isogenic wild-type strain E11 during infection of primary macrophages, grouped into broad functional categories. Within each group, genes are ranked in ascending order by *P*-value. (A). Top 100 annotated genes from the *M. marinum E11* strain that were the most differentially expressed in the *M. marinum* wild-type strain E11 during infection of

primary macrophages. Bar chart of log2-fold changes for individual genes (tags, left). (B). Top 100 annotated genes from the *M. marinum E11* strain that were the most differentially expressed in the *M. marinum eccCb$_1$* transposon mutant compared to the isogenic wild-type strain E11 during infection of primary macrophages (tags, left). Bar chart of log2-fold changes for individual genes.
(PDF)

S6 Fig. Regulation of genes encoding proteins predicted to be involved in metabolic adaptation, energy metabolism and transcriptional regulatory processes in the *M. marinum eccCb$_1$* transposon mutant grown in 7H9 culture medium as well as in the wild-type and eccCb$_1$ transposon mutant strains during infection in human THP-1 macrophages (indicated as 'int') compared to the that in the wild-type strain E11 during growth in 7H9 culture medium. (A) *Catabolism of fatty acids*. Genes were selected based on their annotation and ordered based on expression. (B) Energy generation and NAD$^+$ regeneration. Genes were selected based on their annotation and ordered based on expression. (C) Genes of the *kstR* regulon, which are required for uptake and metabolism of cholesterol [61, 77]. (D) Transcriptional regulation. Genes were selected based on their annotation and ordered based on expression.
(PDF)

S7 Fig. The enriched Gene Ontology (GO) terms of the gene set activated (excluding the *esx-1* locus genes) or repressed by WhiB6. The molecular function GO terms are in red, while the biological process terms are in blue.
(PDF)

Acknowledgments

Author Contributions

Formal analysis: Eveline M. Weerdenburg, Qingtian Guan.

Funding acquisition: Wilbert Bitter, Arnab Pain.

Investigation: Abdallah M. Abdallah, Wilbert Bitter, Arnab Pain.

Methodology: Eveline M. Weerdenburg, Qingtian Guan, Roy Ummels, Stephanie Borggreve, Sabir A. Adroub, Tareq B. Malas, Raeece Naeem, Huoming Zhang, Thomas D. Otto, Wilbert Bitter, Arnab Pain.

Project administration: Abdallah M. Abdallah, Wilbert Bitter, Arnab Pain.

Resources: Wilbert Bitter, Arnab Pain.

Software: Qingtian Guan, Arnab Pain.

Supervision: Abdallah M. Abdallah, Wilbert Bitter, Arnab Pain.

Validation: Eveline M. Weerdenburg.

Visualization: Eveline M. Weerdenburg.

Writing – original draft: Abdallah M. Abdallah.

Writing – review & editing: Abdallah M. Abdallah, Eveline M. Weerdenburg, Qingtian Guan, Wilbert Bitter, Arnab Pain.

References

1. Lewis KN, Liao R, Guinn KM, Hickey MJ, Smith S, Behr MA, et al. Deletion of RD1 from Mycobacterium tuberculosis mimics bacille Calmette-Guerin attenuation. The Journal of infectious diseases. 2003; 187 (1):117–23. https://doi.org/10.1086/345862 PMID: 12508154; PubMed Central PMCID: PMC1458498.

2. Pym AS, Brodin P, Brosch R, Huerre M, Cole ST. Loss of RD1 contributed to the attenuation of the live tuberculosis vaccines Mycobacterium bovis BCG and Mycobacterium microti. Mol Microbiol. 2002; 46 (3):709–17. PMID: 12410828.

3. Stamm LM, Morisaki JH, Gao LY, Jeng RL, McDonald KL, Roth R, et al. Mycobacterium marinum escapes from phagosomes and is propelled by actin-based motility. J Exp Med. 2003; 198(9):1361–8. https://doi.org/10.1084/jem.20031072 PubMed PMID: WOS:000186423700008. PMID: 14597736

4. van der Wel N, Hava D, Houben D, Fluitsma D, van Zon M, Pierson J, et al. M. tuberculosis and M. leprae translocate from the phagolysosome to the cytosol in myeloid cells. Cell. 2007; 129(7):1287–98. https://doi.org/10.1016/j.cell.2007.05.059 PMID: 17604718.

5. Simeone R, Sayes F, Song O, Groschel MI, Brodin P, Brosch R, et al. Cytosolic access of Mycobacterium tuberculosis: critical impact of phagosomal acidification control and demonstration of occurrence in vivo. Plos Pathog. 2015; 11(2):e1004650. Epub 2015/02/07. https://doi.org/10.1371/journal.ppat.1004650 PMID: 25658322; PubMed Central PMCID: PMCPMC4450080.

6. de Jonge MI, Pehau-Arnaudet G, Fretz MM, Romain F, Bottai D, Brodin P, et al. ESAT-6 from Mycobacterium tuberculosis dissociates from its putative chaperone CFP-10 under acidic conditions and exhibits membrane-lysing activity. Journal of bacteriology. 2007; 189(16):6028–34. https://doi.org/10.1128/JB.00469-07 PMID: 17557817; PubMed Central PMCID: PMC1952024.

7. Ma Y, Keil V, Sun J. Characterization of Mycobacterium tuberculosis EsxA membrane insertion: roles of N- and C-terminal flexible arms and central helix-turn-helix motif. The Journal of biological chemistry. 2015; 290(11):7314–22. Epub 2015/02/04. https://doi.org/10.1074/jbc.M114.622076 PMID: 25645924; PubMed Central PMCID: PMCPMC4358149.

8. De Leon J, Jiang G, Ma Y, Rubin E, Fortune S, Sun J. Mycobacterium tuberculosis ESAT-6 exhibits a unique membrane-interacting activity that is not found in its ortholog from non-pathogenic Mycobacterium smegmatis. The Journal of biological chemistry. 2012; 287(53):44184–91. https://doi.org/10.1074/jbc.M112.420869 PMID: 23150662; PubMed Central PMCID: PMC3531734.

9. Coros A, Callahan B, Battaglioli E, Derbyshire KM. The specialized secretory apparatus ESX-1 is essential for DNA transfer in Mycobacterium smegmatis. Molecular microbiology. 2008; 69(4):794–808. https://doi.org/10.1111/j.1365-2958.2008.06299.x PubMed PMID: WOS:000258595000003. PMID: 18554329

10. Ates LS, Brosch R. Discovery of the type VII ESX-1 secretion needle? Mol Microbiol. 2017; 103(1):7–12. Epub 2016/11/20. https://doi.org/10.1111/mmi.13579 PMID: 27859892.

11. Gao LY, Guo S, McLaughlin B, Morisaki H, Engel JN, Brown EJ. A mycobacterial virulence gene cluster extending RD1 is required for cytolysis, bacterial spreading and ESAT-6 secretion. Mol Microbiol. 2004; 53(6):1677–93. https://doi.org/10.1111/j.1365-2958.2004.04261.x PubMed PMID: WOS:000223662100010. PMID: 15341647

12. Hagedorn M, Rohde KH, Russell DG, Soldati T. Infection by tubercular mycobacteria is spread by non-lytic ejection from their amoeba hosts. Science. 2009; 323(5922):1729–33. Epub 2009/03/28. https://doi.org/10.1126/science.1169381 PMID: 19325115; PubMed Central PMCID: PMCPMC2770343.

13. van Leeuwen LM, Boot M, Kuijl C, Picavet DI, van Stempvoort G, van der Pol SMA, et al. Mycobacteria employ two different mechanisms to cross the blood-brain barrier. Cellular microbiology. 2018; 20(9): e12858. Epub 2018/05/12. https://doi.org/10.1111/cmi.12858 PMID: 29749044; PubMed Central PMCID: PMCPMC6175424.

14. van Winden VJC, Ummels R, Piersma SR, Jimenez CR, Korotkov KV, Bitter W, et al. Mycosins Are Required for the Stabilization of the ESX-1 and ESX-5 Type VII Secretion Membrane Complexes. mBio. 2016; 7(5). doi: ARTN e01471-16 https://doi.org/10.1128/mBio.01471-16 PubMed PMID: WOS:000390132900072. PMID: 27795391

15. Phan TH, van Leeuwen LM, Kuijl C, Ummels R, van Stempvoort G, Rubio-Canalejas A, et al. EspH is a hypervirulence factor for Mycobacterium marinum and essential for the secretion of the ESX-1 substrates EspE and EspF. Plos Pathog. 2018; 14(8):e1007247. Epub 2018/08/14. https://doi.org/10.1371/journal.ppat.1007247 PMID: 30102741; PubMed Central PMCID: PMCPMC6107294.

16. Ates LS, Houben EN, Bitter W. Type VII Secretion: A Highly Versatile Secretion System. Microbiol Spectr. 2016; 4(1). Epub 2016/03/22. https://doi.org/10.1128/microbiolspec.VMBF-0011-2015 PMID: 26999398.

17. Groschel MI, Sayes F, Simeone R, Majlessi L, Brosch R. ESX secretion systems: mycobacterial evolution to counter host immunity. Nature reviews Microbiology. 2016; 14(11):677–91. Epub 2016/09/27. https://doi.org/10.1038/nrmicro.2016.131 PMID: 27665717.

18. Fortune SM, Jaeger A, Sarracino DA, Chase MR, Sassetti CM, Sherman DR, et al. Mutually dependent secretion of proteins required for mycobacterial virulence. Proc Natl Acad Sci USA. 2005; 102 (30):10676–81. https://doi.org/10.1073/pnas.0504922102 PubMed PMID: WOS:000230853300049. PMID: 16030141

19. MacGurn JA, Raghavan S, Stanley SA, Cox JS. A non-RD1 gene cluster is required for Snm secretion in Mycobacterium tuberculosis. Molecular microbiology. 2005; 57(6):1653–63. https://doi.org/10.1111/j.1365-2958.2005.04800.x PubMed PMID: WOS:000231610600012. PMID: 16135231

20. Pallen MJ. The ESAT-6/WXG100 superfamily—and a new Gram-positive secretion system? Trends Microbiol. 2002; 10(5):209–12. PMID: 11973144.

21. Daleke MH, Ummels R, Bawono P, Heringa J, Vandenbroucke-Grauls CM, Luirink J, et al. General secretion signal for the mycobacterial type VII secretion pathway. Proceedings of the National Academy of Sciences of the United States of America. 2012; 109(28):11342–7. https://doi.org/10.1073/pnas.1119453109 PMID: 22733768; PubMed Central PMCID: PMC3396530.

22. Daleke MH, Ummels R, Bawono P, Heringa J, Vandenbroucke-Grauls CM, Luirink J, et al. General secretion signal for the mycobacterial type VII secretion pathway. Proc Natl Acad Sci USA. 2012; 109 (28):11342–7. https://doi.org/10.1073/pnas.1119453109 PMID: 22733768; PubMed Central PMCID: PMC3396530.

23. Asensio JA, Arbues A, Perez E, Gicquel B, Martin C. Live tuberculosis vaccines based on phoP mutants: a step towards clinical trials. Expert opinion on biological therapy. 2008; 8(2):201–11. https://doi.org/10.1517/14712598.8.2.201 PMID: 18194076.

24. Broset E, Martin C, Gonzalo-Asensio J. Evolutionary landscape of the Mycobacterium tuberculosis complex from the viewpoint of PhoPR: implications for virulence regulation and application to vaccine development. mBio. 2015; 6(5):e01289–15. Epub 2015/10/23. https://doi.org/10.1128/mBio.01289-15 PMID: 26489860; PubMed Central PMCID: PMCPMC4620462.

25. Walters SB, Dubnau E, Kolesnikova I, Laval F, Daffe M, Smith I. The Mycobacterium tuberculosis PhoPR two-component system regulates genes essential for virulence and complex lipid biosynthesis. Mol Microbiol. 2006; 60(2):312–30. https://doi.org/10.1111/j.1365-2958.2006.05102.x PMID: 16573683.

26. Abramovitch RB, Rohde KH, Hsu FF, Russell DG. aprABC: a Mycobacterium tuberculosis complex-specific locus that modulates pH-driven adaptation to the macrophage phagosome. Molecular microbiology. 2011; 80(3):678–94. https://doi.org/10.1111/j.1365-2958.2011.07601.x PubMed PMID: WOS:000289729800012. PMID: 21401735

27. Gordon BRG, Li YF, Wang LR, Sintsova A, van Bakel H, Tian SH, et al. Lsr2 is a nucleoid-associated protein that targets AT-rich sequences and virulence genes in Mycobacterium tuberculosis (vol 107, pg 5154, 2010). Proc Natl Acad Sci USA. 2010; 107(43):18741-. https://doi.org/10.1073/Pnas.1014494107 PubMed PMID: WOS:000283677400093.

28. Pang XH, Samten B, Cao GX, Wang XS, Tvinnereim AR, Chen XL, et al. MprAB regulates the espA operon in mycobacterium tuberculosis and modulates ESX-1 function and host cytokine response. Journal of bacteriology. 2013; 195(1):66–75. https://doi.org/10.1128/JB.01067-12 PubMed PMID: WOS:000316959000010. PMID: 23104803

29. Raghavan S, Manzanillo P, Chan K, Dovey C, Cox JS. Secreted transcription factor controls Mycobacterium tuberculosis virulence. Nature. 2008; 454(7205):717–21. https://doi.org/10.1038/nature07219 PMID: 18685700; PubMed Central PMCID: PMC2862998.

30. Rickman L, Scott C, Hunt DM, Hutchinson T, Menendez MC, Whalan R, et al. A member of the cAMP receptor protein family of transcription regulators in Mycobacterium tuberculosis is required for virulence in mice and controls transcription of the rpfA gene coding for a resuscitation promoting factor. Molecular microbiology. 2005; 56(5):1274–86. https://doi.org/10.1111/j.1365-2958.2005.04609.x PubMed PMID: WOS:000228975300014. PMID: 15882420

31. van der Sar AM, Abdallah AM, Sparrius M, Reinders E, Vandenbroucke-Grauls CMJE, Bitter W. Mycobacterium marinum strains can be divided into two distinct types based on genetic diversity and virulence. Infection and immunity. 2004; 72(11):6306–12. https://doi.org/10.1128/IAI.72.11.6306-6312.2004 PubMed PMID: WOS:000224664300016. PMID: 15501758

32. Weerdenburg EM, Abdallah AM, Rangkuti F, Abd El Ghany M, Otto TD, Adroub SA, et al. Genome-wide transposon mutagenesis indicates that Mycobacterium marinum customizes its virulence

mechanisms for survival and replication in different hosts. Infection and immunity. 2015; 83(5):1778–88. Epub 2015/02/19. https://doi.org/10.1128/IAI.03050-14 PMID: 25690095; PubMed Central PMCID: PMCPMC4399070.

33. Stoop EJ, Schipper T, Rosendahl Huber SK, Nezhinsky AE, Verbeek FJ, Gurcha SS, et al. Zebrafish embryo screen for mycobacterial genes involved in the initiation of granuloma formation reveals a newly identified ESX-1 component. Dis Model Mech. 2011; 4(4):526–36. Epub 2011/03/05. https://doi.org/10.1242/dmm.006676 PMID: 21372049; PubMed Central PMCID: PMCPMC3124061.

34. Abdallah AM, Verboom T, Weerdenburg EM, van Pittius NCG, Mahasha PW, Jimenez C, et al. PPE and PE_PGRS proteins of Mycobacterium marinum are transported via the type VII secretion system ESX-5. Mol Microbiol. 2009; 73(3):329–40. https://doi.org/10.1111/j.1365-2958.2009.06783.x PubMed PMID: WOS:000268792700002. PMID: 19602152

35. Groschel MI, Sayes F, Shin SJ, Frigui W, Pawlik A, Orgeur M, et al. Recombinant BCG Expressing ESX-1 of Mycobacterium marinum Combines Low Virulence with Cytosolic Immune Signaling and Improved TB Protection. Cell Rep. 2017; 18(11):2752–65. Epub 2017/03/16. https://doi.org/10.1016/j.celrep.2017.02.057 PMID: 28297677.

36. Bardarov S, Bardarov S, Pavelka MS, Sambandamurthy V, Larsen M, Tufariello J, et al. Specialized transduction: an efficient method for generating marked and unmarked targeted gene disruptions in Mycobacterium tuberculosis, M-bovis BCG and M-smegmatis. Microbiol-Sgm. 2002; 148:3007–17. https://doi.org/10.1099/00221287-148-10-3007 PubMed PMID: WOS:000178588300011. PMID: 12368434

37. Sambandamurthy VK, Derrick SC, Hsu T, Chen B, Larsen MH, Jalapathy KV, et al. Mycobacterium tuberculosis DeltaRD1 DeltapanCD: a safe and limited replicating mutant strain that protects immuno-competent and immunocompromised mice against experimental tuberculosis. Vaccine. 2006; 24(37–39):6309–20. https://doi.org/10.1016/j.vaccine.2006.05.097 PMID: 16860907.

38. Sambandamurthy VK, Derrick SC, Jalapathy KV, Chen B, Russell RG, Morris SL, et al. Long-term pro-tection against tuberculosis following vaccination with a severely attenuated double lysine and panto-thenate auxotroph of Mycobacterium tuberculosis. Infection and immunity. 2005; 73(2):1196–203. https://doi.org/10.1128/IAI.73.2.1196-1203.2005 PMID: 15664964; PubMed Central PMCID: PMC547051.

39. Levene MJ, Korlach J, Turner SW, Foquet M, Craighead HG, Webb WW. Zero-mode waveguides for single-molecule analysis at high concentrations. Science. 2003; 299(5607):682–6. https://doi.org/10.1126/science.1079700 PubMed PMID: WOS:000180687700039. PMID: 12560545

40. Chin CS, Alexander DH, Marks P, Klammer AA, Drake J, Heiner C, et al. Nonhybrid, finished microbial genome assemblies from long-read SMRT sequencing data. Nature methods. 2013; 10(6):563-+. https://doi.org/10.1038/nmeth.2474 PubMed PMID: WOS:000319668700028. PMID: 23644548

41. Otto TD, Sanders M, Berriman M, Newbold C. Iterative Correction of Reference Nucleotides (iCORN) using second generation sequencing technology. Bioinformatics. 2010; 26(14):1704–7. https://doi.org/10.1093/bioinformatics/btq269 PubMed PMID: WOS:000279474400004. PMID: 20562415

42. Otto TD, Dillon GP, Degrave WS, Berriman M. RATT: rapid annotation transfer tool. Nucleic Acids Res. 2011; 39(9):e57. doi: ARTN e57 https://doi.org/10.1093/nar/gkq1268 PubMed PMID: WOS:000290589500002. PMID: 21306991

43. Manganelli R, Dubnau E, Tyagi S, Kramer FR, Smith I. Differential expression of 10 sigma factor genes in Mycobacterium tuberculosis. Molecular microbiology. 1999; 31(2):715–24. PMID: 10027986.

44. Quinlan AR, Hall IM. BEDTools: a flexible suite of utilities for comparing genomic features. Bioinformat-ics. 2010; 26(6):841–2. https://doi.org/10.1093/bioinformatics/btq033 PubMed PMID: WOS:000275243500019. PMID: 20110278

45. Anders S, Huber W. Differential expression analysis for sequence count data. Genome biology. 2010; 11(10):R106. https://doi.org/10.1186/gb-2010-11-10-r106 PMID: 20979621; PubMed Central PMCID: PMC3218662.

46. Carlsson F, Joshi SA, Rangell L, Brown EJ. Polar localization of virulence-related Esx-1 secretion in mycobacteria. Plos Pathog. 2009; 5(1):e1000285. https://doi.org/10.1371/journal.ppat.1000285 PMID: 19180234; PubMed Central PMCID: PMC2628743.

47. Abdallah AM, Hill-Cawthorne GA, Otto TD, Coll F, Guerra-Assuncao JA, Gao G, et al. Genomic expres-sion catalogue of a global collection of BCG vaccine strains show evidence for highly diverged meta-bolic and cell-wall adaptations. Sci Rep. 2015; 5:15443. https://doi.org/10.1038/srep15443 PMID: 26487098.

48. Zhu J, Zhang HM, Guo TN, Li WY, Li HY, Zhu Y, et al. Quantitative proteomics reveals differential bio-logical processes in healthy neonatal cord neutrophils and adult neutrophils. Proteomics. 2014; 14(13–14):1688–97. https://doi.org/10.1002/pmic.201400009 PubMed PMID: WOS:000339553900012. PMID: 24782442

49. Shadforth IP, Dunkley TPJ, Lilley KS, Bessant C. i-Tracker: For quantitative proteomics using iTRAQ (TM). Bmc Genomics. 2005; 6:145. doi: Artn 145 https://doi.org/10.1186/1471-2164-6-145 PubMed PMID: WOS:000232982200001. PMID: 16242023

50. Waldbauer JR, Rodrigue S, Coleman ML, Chisholm SW. Transcriptome and proteome dynamics of a light-dark synchronized bacterial cell cycle. Plos One. 2012; 7(8):e43432. https://doi.org/10.1371/journal.pone.0043432 PMID: 22952681; PubMed Central PMCID: PMC3430701.

51. Joshi SA, Ball DA, Sun MG, Carlsson F, Watkins BY, Aggarwal N, et al. EccA1, a component of the Mycobacterium marinum ESX-1 protein virulence factor secretion pathway, regulates mycolic acid lipid synthesis. Chem Biol. 2012; 19(3):372–80. https://doi.org/10.1016/j.chembiol.2012.01.008 PMID: 22444592.

52. Jamwal SV, Mehrotra P, Singh A, Siddiqui Z, Basu A, Rao KVS. Mycobacterial escape from macrophage phagosomes to the cytoplasm represents an alternate adaptation mechanism. Sci Rep-Uk. 2016; 6. doi: ARTN 23089 https://doi.org/10.1038/srep23089 PubMed PMID: WOS:000372054800001. PMID: 26980157

53. Houben D, Demangel C, van Ingen J, Perez J, Baldeon L, Abdallah AM, et al. ESX-1-mediated translocation to the cytosol controls virulence of mycobacteria. Cellular microbiology. 2012; 14(8):1287–98. https://doi.org/10.1111/j.1462-5822.2012.01799.x PMID: 22524898.

54. Weston A, Stern RJ, Lee RE, Nassau PM, Monsey D, Martin SL, et al. Biosynthetic origin of mycobacterial cell wall galactofuranosyl residues. Tubercle and lung disease: the official journal of the International Union against Tuberculosis and Lung Disease. 1997; 78(2):123–31. PMID: 9692181.

55. Pastoret S, Fraipont C, den Blaauwen T, Wolf B, Aarsman ME, Piette A, et al. Functional analysis of the cell division protein FtsW of Escherichia coli. Journal of bacteriology. 2004; 186(24):8370–9. https://doi.org/10.1128/JB.186.24.8370-8379.2004 PMID: 15576787; PubMed Central PMCID: PMC532424.

56. Schmidt KL, Peterson ND, Kustusch RJ, Wissel MC, Graham B, Phillips GJ, et al. A predicted ABC transporter, FtsEX, is needed for cell division in Escherichia coli. Journal of bacteriology. 2004; 186 (3):785–93. https://doi.org/10.1128/JB.186.3.785-793.2004 PubMed PMID: WOS:000188371600023. PMID: 14729705

57. McKinney JD, Honer zu Bentrup K, Munoz-Elias EJ, Miczak A, Chen B, Chan WT, et al. Persistence of Mycobacterium tuberculosis in macrophages and mice requires the glyoxylate shunt enzyme isocitrate lyase. Nature. 2000; 406(6797):735–8. https://doi.org/10.1038/35021074 PMID: 10963599.

58. Munoz-Elias EJ, McKinney JD. Mycobacterium tuberculosis isocitrate lyases 1 and 2 are jointly required for in vivo growth and virulence. Nature medicine. 2005; 11(6):638–44. https://doi.org/10.1038/nm1252 PMID: 15895072; PubMed Central PMCID: PMC1464426.

59. Liu KY, Yu JZ, Russell DG. pckA-deficient Mycobacterium bovis BCG shows attenuated virulence in mice and in macrophages. Microbiol-Sgm. 2003; 149:1829–35. https://doi.org/10.1099/mic/.0.26234–0 PubMed PMID: WOS:000184209000022.

60. Marrero J, Rhee KY, Schnappinger D, Pethe K, Ehrt S. Gluconeogenic carbon flow of tricarboxylic acid cycle intermediates is critical for Mycobacterium tuberculosis to establish and maintain infection. Proc Natl Acad Sci USA. 2010; 107(21):9819–24. https://doi.org/10.1073/pnas.1000715107 PubMed PMID: WOS:000278054700062. PMID: 20439709

61. Kendall SL, Withers M, Soffair CN, Moreland NJ, Gurcha S, Sidders B, et al. A highly conserved transcriptional repressor controls a large regulon involved in lipid degradation in Mycobacterium smegmatis and Mycobacterium tuberculosis. Mol Microbiol. 2007; 65(3):684–99. https://doi.org/10.1111/j.1365-2958.2007.05827.x PMID: 17635188; PubMed Central PMCID: PMC1995591.

62. Brodin P, Majlessi L, Marsollier L, de Jonge MI, Bottai D, Demangel C, et al. Dissection of ESAT-6 system 1 of Mycobacterium tuberculosis and impact on immunogenicity and virulence. Infection and immunity. 2006; 74(1):88–98. https://doi.org/10.1128/IAI.74.1.88-98.2006 PMID: 16368961; PubMed Central PMCID: PMC1346617.

63. Daleke MH, van der Woude AD, Parret AHA, Ummels R, de Groot AM, Watson D, et al. Specific chaperones for the type VII Protein secretion pathway. The Journal of biological chemistry. 2012; 287 (38):31939–47. https://doi.org/10.1074/jbc.M112.397596 PubMed PMID: WOS:000309059400033. PMID: 22843727

64. Sani M, Houben EN, Geurtsen J, Pierson J, de Punder K, van Zon M, et al. Direct visualization by cryo-EM of the mycobacterial capsular layer: a labile structure containing ESX-1-secreted proteins. Plos Pathog. 2010; 6(3):e1000794. https://doi.org/10.1371/journal.ppat.1000794 PMID: 20221442; PubMed Central PMCID: PMC2832766.

65. Zhang M, Chen JM, Sala C, Rybniker J, Dhar N, Cole ST. EspI regulates the ESX-1 secretion system in response to ATP levels in Mycobacterium tuberculosis. Mol Microbiol. 2014; 93(5):1057–65. https://doi.org/10.1111/mmi.12718 PubMed PMID: WOS:000341639600015. PMID: 25039394

66. Zheng F, Long Q, Xie J. The function and regulatory network of WhiB and WhiB-like protein from comparative genomics and systems biology perspectives. Cell Biochem Biophys. 2012; 63(2):103–8. https://doi.org/10.1007/s12013-012-9348-z PMID: 22388511.

67. Das C, Ghosh TS, Mande SS. Computational analysis of the ESX-1 region of Mycobacterium tuberculosis: insights into the mechanism of type VII secretion system. Plos One. 2011; 6(11):e27980. https://doi.org/10.1371/journal.pone.0027980 PMID: 22140496; PubMed Central PMCID: PMC3227618.

68. Bosserman RE, Nguyen TT, Sanchez KG, Chirakos AE, Ferrell MJ, Thompson CR, et al. WhiB6 regulation of ESX-1 gene expression is controlled by a negative feedback loop in Mycobacterium marinum. Proc Natl Acad Sci USA. 2017; 114(50):E10772–E81. https://doi.org/10.1073/pnas.1710167114 PMID: 29180415; PubMed Central PMCID: PMCPMC5740670.

69. Chen Z, Hu Y, Cumming BM, Lu P, Feng L, Deng J, et al. Mycobacterial WhiB6 Differentially Regulates ESX-1 and the Dos Regulon to Modulate Granuloma Formation and Virulence in Zebrafish. Cell Rep. 2016; 16(9):2512–24. https://doi.org/10.1016/j.celrep.2016.07.080 PMID: 27545883.

70. Solans L, Aguilo N, Samper S, Pawlik A, Frigui W, Martin C, et al. A specific polymorphism in mycobacterium tuberculosis H37Rv causes differential ESAT-6 expression and identifies WhiB6 as a novel ESX-1 component. Infection and immunity. 2014; 82(8):3446–56. https://doi.org/10.1128/IAI.01824-14 PubMed PMID: WOS:000339161400033. PMID: 24891105

71. Abdallah AM, Verboom T, Weerdenburg EM, van Pittius NCG, Mahasha PW, Jimenez C, et al. PPE and PE_PGRS proteins of Mycobacterium marinum are transported via the type VII secretion system ESX-5. Molecular microbiology. 2009; 73(3):329–40. https://doi.org/10.1111/j.1365-2958.2009.06783.x PubMed PMID: WOS:000268792700002. PMID: 19602152

72. Ates LS, Dippenaar A, Ummels R, Piersma SR, van der Woude AD, van der Kuij K, et al. Mutations in ppe38 block PE_PGRS secretion and increase virulence of Mycobacterium tuberculosis. Nat Microbiol. 2018; 3(2):181–8. Epub 2018/01/18. https://doi.org/10.1038/s41564-017-0090-6 PMID: 29335553.

73. Cao G, Howard ST, Zhang P, Wang X, Chen XL, Samten B, et al. EspR, a regulator of the ESX-1 secretion system in Mycobacterium tuberculosis, is directly regulated by the two-component systems MprAB and PhoPR. Microbiology. 2015; 161(Pt 3):477–89. Epub 2014/12/30. https://doi.org/10.1099/mic.0.000023 PMID: 25536998.

74. Hunt DM, Sweeney NP, Mori L, Whalan RH, Comas I, Norman L, et al. Long-range transcriptional control of an operon necessary for virulence-critical ESX-1 secretion in Mycobacterium tuberculosis. Journal of bacteriology. 2012; 194(9):2307–20. Epub 2012/03/06. https://doi.org/10.1128/JB.00142-12 PMID: 22389481; PubMed Central PMCID: PMCPMC3347062.

75. den Hengst CD, Buttner MJ. Redox control in actinobacteria. Biochim Biophys Acta. 2008; 1780 (11):1201–16. https://doi.org/10.1016/j.bbagen.2008.01.008 PubMed PMID: WOS:000259359600003. PMID: 18252205

76. Ates LS, van der Woude AD, Bestebroer J, van Stempvoort G, Musters RJ, Garcia-Vallejo JJ, et al. The ESX-5 System of Pathogenic Mycobacteria Is Involved In Capsule Integrity and Virulence through Its Substrate PPE10. Plos Pathog. 2016; 12(6):e1005696. Epub 2016/06/10. https://doi.org/10.1371/journal.ppat.1005696 PMID: 27280885; PubMed Central PMCID: PMCPMC4900558.

77. Mohn WW, van der Geize R, Stewart GR, Okamoto S, Liu J, Dijkhuizen L, et al. The actinobacterial mce4 locus encodes a steroid transporter. The Journal of biological chemistry. 2008; 283(51):35368–74. https://doi.org/10.1074/jbc.M805496200 PMID: 18955493.